A Single Stage 1.65kW AC-DC LLC Converter with Power Factor Correction (PFC) for On-Board Charger (OBC) Application

Wenbo Liu, Andrew Yurek, Bo Sheng, Yang Chen, Yan-Fei Liu, *Fellow, IEEE* and Paresh. C. Sen, *Life Fellow, IEEE*

Department of Electrical and Computer Engineering
Queen's University, Kingston, Canada
liu.wenbo@queensu.ca, yanfei.liu@queensu.ca

Abstract — **A single stage 1.65kW AC-DC LLC converter with Power Factor Correction (PFC) for OBC application is proposed. A boost inductor is not required since the LLC converter serves as both the AC-DC and DC-DC stage which provides all the functions of rectification, PFC, output voltage regulation and galvanic isolation. A design methodology is proposed in this paper to maintain the output voltage regulation and PFC over the entire AC input voltage range from zero to peak voltage. Benefiting from the true-single-stage structure, the quantity of active switches and magnetic components is reduced. Therefore, high power density and high efficiency can be achieved with an overall reduction in the number of components. An experimental prototype is designed based on the LLC PFC design methodology. Stable DC output voltage regulation is implemented with over 99% Power Factor. Experimental testing is conducted which achieves over 2.9kW/L power density and 96.9% overall efficiency.**

Keywords – Power Factor Correction (PFC), single stag, LLC resonant converter

I. INTRODUCTION

Research and development of electric vehicles (EVs) technologies are becoming more popular, and the worldwide EV market is growing steadily. For the power supply systems on EVs, the on-board charger (OBC) which charges the high voltage battery (250V to 430V) is considered as the most critical part. Increasing power ratings of OBC at 6.6kW, 11kW and 22kW allow faster battery charging to significantly improve the performance of EVs [1]. At the meanwhile problems are imposed: more compact topology structure, lighter converter weight and lower temperature rise of the OBC are needed to maintain the environment on vehicles. The power factor (PF) requirement of input current harmonics also limits the design and control schemes, adding on cost and size of OBCs.

Conventional OBC structure uses an AC-DC Boost converter with Power Factor Correction (PFC), followed by a DC-DC isolated power converter to charge the battery in EVs [2][3]. The two-stage structure with many components limits the power density and efficiency performance [4][5]. Literatures have proposed both designs of novel topologies and wide bandgap (WBG) devices to improve performance of OBC. Development of WBG devices allow the converters to operate at significantly higher switching frequency to reduce the size of magnetic components [6][7][8]. A bridgeless totem pole PFC with WBG device followed by an LLC DC-DC converter has become a mainstream of OBC study. The bridgeless two-stage structure uses less semiconductor switches and can achieve higher efficiency and smaller size [9][10].

However, these researches contribute to reduce the quantity of switches, but the magnetic components, especially the bulky Boost inductor still cannot be avoided [11]. In the state-of-art researches, the overall efficiency of OBC based on Totem pole PFC + LLC converter structure as shown in Fig. 1 is limited below 96%. With complicated magnetic components design and other down-sizing methods, the maximum power density can achieve 2.4kW/L.

A single stage LLC based AC/DC converter as shown in Fig. 2 is proposed for OBC application in this paper. In most of the research, the LLC converter is considered as the DC/DC stage instead of AC/DC stage [12][13]. The proposed OBC in contrast achieves both AC/DC stage with PFC and DC/DC voltage regulation stage with one LLC converter [14][15]. The LLC OBC essentially removes the bulky PFC inductor and reduces the number of switches, which saves considerable volume and further increases power density.

In the proposed LLC AC/DC converter, no Boost inductor is needed in the on-board charger system. The LLC converter serves as both the AC-DC and DC-DC stage which provides all the functions of rectification, power factor correction and galvanic isolation as well as voltage regulation. This paper is organized as follows: Section II proposes a DC static averaging method to analyze the losses of the PFC. Section III demonstrates the design criteria of LLC converter resonant tank to implement the PFC functions in the complete voltage range. Then, the implementation of LLC OBC prototype and the experimental result are shown in section IV. Section V concludes the paper.
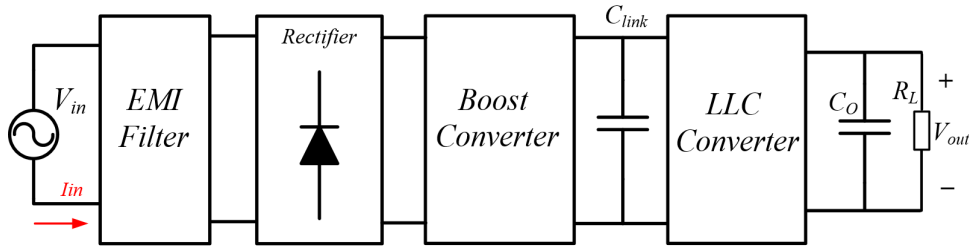
4594

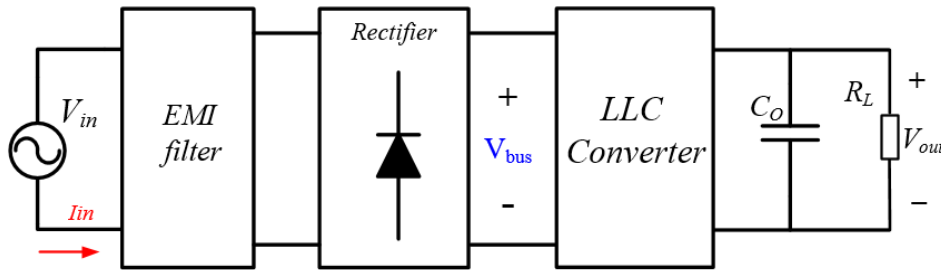Fig. 1. Conventional two stage Boost PFC & LLC OBC.

Fig. 2. Proposed OBC based on single stage LLC converter.

II. FULL VOLTAGE RANGE LLC RESONANT TANK DESIGN

This section demonstrates the design criterion of the LLC AC-DC converter with PFC. The maximum output power is designed to be 1650W. Four such LLC PFC converters can be paralleled to achieve a 6.6kW 4-phase converter for OBC application with decreased current stress on the components [16][17]. The power rating and input/output voltage specifications imposes specific requirements for the LLC resonant tank including Lr, Lp, Cr and transformer turns ratio N selection.

A. Quasi - Static DC Operating Point Analysis

To meet power factor correction operation, in the entire AC input range, the LLC converter must have enough voltage boosting capability to keep a stable output voltage with AC input ranging from zero to peak voltage [106][107]. This section uses quasi-static DC operating point to analyze the voltage gain by assuming the AC line cycle is divided into many small elements corresponding different phase angles, the operation in each element is considered as DC-DC static operation [18][19].

The specifications of the LLC PFC stage are shown in Table 7.1. Full power is provided from 330V to 430V output voltage, and the output power is de-rated between 250V to 330V output with 5A load current at maximum.

To analyze the quasi-static operation, the instantaneous input voltage and power are calculated at the static points. The instantaneous AC input voltage V_{bus} is (1):

TABLE I. PARAMETERS OF THE STUDIED LLC CONVERTER

Output Power Po	Input Voltage Vin (RMS)	Output Voltage Vo	Switching Frequency fs
1.65kW	200V ~ 240V	250V ~ 430V	350kHz ~ 650kHz

$$V_{bus}(\theta) = \sqrt{2}V_{in}sin\theta \quad (1)$$

To achieve PFC operation, the input current is required to be sinusoidal in phase with the input voltage, so the instantaneous power P_{ac} is defined in (7.2):

$$P_{ac}(\theta) = \sqrt{2}V_{in}sin\theta \cdot \sqrt{2}I_{in}sin\theta = 2P_osin^2\theta \quad (2)$$

Where θ is the phase angle ranges from 0° to 180°; V_{in} and I_{in} are the root mean square (RMS) values of AC input voltage and current respectively. Fig. 3 shows the plots of V_{bus}, required voltage gain G_{req} and instantaneous input power P_{ac}.
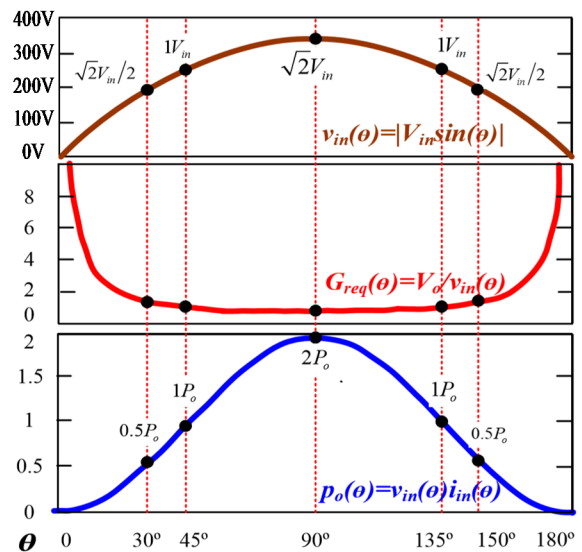

Fig. 3. General voltage gain requirement of AC-DC converter

Phase angle θ	Input voltage (V)	Input current (A)	Load resistance (Ω)	Output power (W)
90°	311	10.6	33	3300
75°	300	10.2	35	3079
60°	269	9.2	44	2475
45°	220	7.5	66	1650
30°	155	5.3	132	825
15°	80	2.7	493	221

According to Fig. 3, the instantaneous input power is changing with the phase angle. As the output voltage is constant, the instantaneous equivalent output current is changing, so the instantaneous equivalent load resistance is also changing with phase angle [20][21]. Table II shows six conditions with 220V AC input and 330V DC output at 5A load current:

(1) At 90° condition, the input voltage, input current and instantaneous power are at maximum, the power is $2P_o$ (3300W), instantaneous load resistance is 33Ω (330V/10A).

(2) At 75° condition, the power is 3079W, load resistance is 35Ω (330V/9.32A).

(3) At 60° condition, the power is 2475W, load resistance is 44Ω (330V/7.5A).

(4) At 45°, input voltage and power are at average value, instantaneous power is P_o (1650W), load resistance is 66Ω (330V/5A). This is half load condition.

(5) At 30°, the instantaneous power is 825W, load resistance is 132Ω (330V/7.5A).

(6) At 15°, input voltage is 80V, the power is 221W, load resistance is 493Ω (330V/0.67A). This is a light load condition with high instantaneous load resistance.

When the phase angle is changing from 90° to 0°, the input voltage keeps decreasing. To regulate the output voltage and keep the stability, the voltage gain requirement keeps increasing. However, the load is also becoming lighter when the phase angle is decreasing. LLC converter has much higher voltage gain at light load than heavy load. Therefore, the LLC converter has the potential to achieve the PFC operation which also requires higher voltage gain at lighter load condition. Thus, two design criterions are needed: (1) The LLC converter must satisfy the quasi-static operation at peak voltage and peak power, at which point the phase angle is the 90°. (2) The LLC converter must satisfy all the other phase angles from 1° to 89°.

It is noted that the actual output voltage is a DC value with a small double line frequency voltage ripple ($\pm$10V ripple at 120Hz with 330V DC voltage). The actual output power is a DC value, and the difference of output power and instantaneous power is buffered by the output electrolytic capacitors.

B. Implementation of Peak Power Condition

To first implement the peak power condition which occurs at 90° when both input voltage and input current are at the peak, L_r, L_p, C_r parameters and transformer turns ratio N are selected. The transformer primary and secondary turns ratio $N=N_{pri}:N_{sec}$ is first determined since the converter is designed to operate below resonant frequency. Therefore, the minimum voltage gain of LLC is determined to be 1, which corresponds to the minimum output voltage at maximum input voltage condition. So N is determined by (3):

$$N = \sqrt{2}V_{in\_max}/V_{o\_min} = 339:250 \qquad (3)$$

To implement the winding configuration with PQ3535 core size, the primary side is selected to be 23 turns and the secondary side is selected to be 17 turns. The resonant inductor L_r, parallel inductor L_p and resonant capacitor C_r are determined by the higher resonant frequency f_{r1}, lower resonant frequency f_{r2} and maximum required voltage gain (at peak power condition) G_{req_pk}, based on equation (4) and (5):

$$f_{r1} = \frac{1}{2\pi\sqrt{L_rC_r}} \quad , \quad f_{r2} = \frac{1}{2\pi\sqrt{(L_r+L_p)C_r}} \qquad (4)$$

$$G_{req\_pk} = \frac{N \cdot V_{o\_max}}{\sqrt{2}V_{in\_min}} = \frac{V_{in\_max} \cdot V_{o\_max}}{V_{in\_min} \cdot V_{o\_min}} \qquad (5)$$

So G_{req_pk} is equal to 2.1 based on the input and output voltage requirements. Since the maximum frequency is set to be f_{r1}, the minimum frequency is set to be f_{r2} and the required voltage gain can be calculated, the values of L_r, L_p and C_r can be determined according to the design algorithm from previous research. The resonant parameters for peak load DC static operating points that can meet the peak power voltage gain requirement are therefore decided as shown in Table III.

C. Implementation of Entire AC Input Range (0° to 180°)

For any AC input RMS voltage V_{in} from 200Vac to 240Vac, DC output voltage V_o should be regulated in the entire AC line cycle, hence enough voltage gain G_{req} is required at any phase to maintain the regulation of V_o [22][23]. The value of G_{req} is determined in (6):

$$G_{req}(\theta) = N \frac{V_o}{V_{bus}(\theta)} = \frac{N \cdot V_o}{\sqrt{2}V_{in}\sin\theta} \qquad (6)$$

TABLE III. PARAMETERS TO MEET PEAK POWER CONDITION

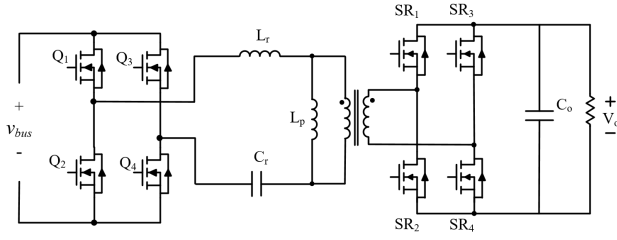| Lr Value	Lp Value	Cr Value	Tx Turns Ratio
8.5uH	21uH	7nF	23:17

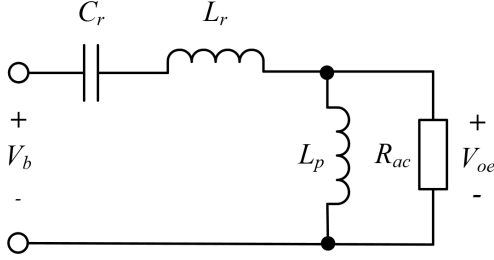Fig. 4. LLC converter of PFC stage after rectifier

Fig. 5. Equivalent RLC circuit of LLC converter

With PFC operation, both the peak voltage and peak power occur at 90° phase, and no load condition occurs at 0° and 180°. Therefore, as shown by the red curve in Fig. 3, the voltage gain has a minimum requirement at peak input voltage and power at 90°. By defining the minimum gain as G_{req_min}, the peak power gain requirement $G_{req\_pk} = G_{req\_min}$, the required gain function of phase angle θ is (7):

$$G_{req}(\theta) = \frac{G_{req_{pk}}}{sin\theta} \qquad (7)$$

As discussed previously in the paper, to meet the voltage gain requirement of all peak power conditions at 90° of any AC input voltage and DC output voltage, G_{req_pk} must satisfy equation (5) and the resonant parameters can be designed based on G_{req_pk}. To analyze the properties of the LLC converter shown in Fig. 4, define $k = L_p / L_r$. In the equivalent circuit shown in Fig. 5, the average equivalent resistance R_e is (8):

$$R_e = \frac{V_{oe}}{I_{oe}} = \frac{2\sqrt{2}NV_o/\pi}{\pi I_o/2\sqrt{2}N} = \frac{8N^2}{\pi^2}R_L \qquad (8)$$

Where R_L is the average load resistance. For instantaneous power with respect to AC line, the equivalent resistance at different θ is (9):

$$R_{ac}(\theta) = \frac{V_{oe}^2}{P(\theta)} = R_e\frac{P}{P(\theta)} = \frac{4N^2R_L}{\pi^2 sin^2\theta} \qquad (9)$$

The voltage gain of LLC versus switching frequency f_s is in (10):

$$G(f_s) = \frac{V_{oe}}{V_b} = \frac{L_p(j2\pi f_s)//R_{ac}}{L_r(j2\pi f_s) + 1/C_r(j2\pi f_s) + L_p(j2\pi f_s)//R_{ac}} =$$
$$\frac{L_pC_rR_{ac}(2\pi f_s)^2}{L_rC_rL_p(j2\pi f_s)^3 + (L_p+L_r)C_rR_{ac}(j2\pi f_s)^2 + L_p(j2\pi f_s) + R_{ac}} \qquad (10)$$

Define the resonant angular frequency $\omega_r = 2\pi f_{r1}$. And define the quality factor: $Q(\theta) = \frac{\omega r L_r}{R_{ac}(\theta)} = Q_0 sin^2\theta$, the average quality factor is $Q_0 = \frac{\omega_r L_r}{R_L} \cdot \frac{\pi^2}{8N^2}$.

Substitute the equations (5) to (9) into the voltage gain equation (10) and obtain the expression of voltage gain versus f_s and θ in (11):

$$G(f_s) = \frac{1}{1 + \frac{1}{k}\left(1 - \frac{f_{r1}^2}{f_s^2}\right) + j2Q_0 sin^2\theta(\frac{f_s}{f_{r1}} - \frac{f_{r1}}{f_s})} \qquad (11)$$

The amplitude of the voltage gain versus f_s and θ is in (12):

$$M(f_s) = \frac{1}{\sqrt{\left(1 + \frac{1}{k}\left(1 - \frac{f_{r1}^2}{f_s^2}\right)\right)^2 + 4Q_0^2 sin^4\theta\left(\frac{f_s}{f_{r1}} - \frac{f_{r1}}{f_s}\right)^2}} \qquad (12)$$

In the proposed LLC converter, f_s is always between f_{s2} and f_{s1}. The voltage gain at f_{r2} is the maximum gain at no load condition, and at high load condition, the gain at f_{r2} is close to maximum voltage gain. Therefore, voltage gain at f_{r2} is used to justify if the converter meets the gain requirement. Calculate the voltage gain at $f_s = f_{r2}$ at different θ in (13):

$$M_{fr2}(\theta) = \frac{1}{\sqrt{\frac{4Q_0^2 sin^4\theta * k^2}{1+k}}} = \frac{1}{\sqrt{4Q_0^2 * k^2/(1+k)}} * \frac{1}{sin^2\theta} \qquad (13)$$

Assume the LLC converter can provide enough voltage gain at f_{r2} at peak input voltage and peak power condition ($P_{ac} = 2P_o$, $\theta = 90°$), the peak voltage gain is equal to M_{fr2} at 90°. Derive the relation of G_{req_pk} and $M_{fr2}(90°)$ in (14)

$$G_{req\_pk} = M_{fr2}(90°) = \frac{1}{\sqrt{4Q_0^2 * k^2/(1+k)}} \qquad (14)$$

Substrate equation (7.7) and (7.13) into (7.14). Since $sin^2\theta \le sin\theta$ is always true for whatever phase angle θ, equation (7.15) can be achieved:

$$G_{req}(\theta) = \frac{G_{req\_pk}}{sin\theta} \le \frac{G_{req\_pk}}{sin^2\theta} = \frac{1}{\sqrt{\frac{4Q_0^2 * k^2}{1+k}}} * \frac{1}{sin^2\theta} = M_{fr2}(\theta)$$
$$(14)$$

Therefore, the converter will always satisfy $G_{req}(\theta) \le M_{fr2}(\theta)$ from 0° to 180° if the voltage gain requirement at peak input voltage and power is satisfied at f_{r2}. The voltage gain requirement in the entire AC voltage range is always no bigger than the voltage gain achieved at f_{r2}. This conclusion indicates that the voltage boost ability of LLC increases faster than voltage gain requirement when instantaneous power is getting smaller.

Thus, an AC-DC LLC converter can be designed to achieve perfect power factor correction to implement the voltage gain requirement for output voltage regulation. By selecting L_r, L_p and C_r to achieve enough voltage gain at peak

4597

voltage ($V_{bus} = \sqrt{2}V_{in\_min}$) and peak power ($P_{ac} = 2P_o$) condition, the LLC converter will be able to provide enough voltage gain at all the other AC phase angle.

Based on the fundamental input and output specifications as shown in Table 2, an LLC converter is designed. With the structure shown in Fig. 4, a GaN FET full bridge is used for LLC stage and a MOSFET full bridge is employed as synchronous rectifier (SR) for the secondary side DC voltage output. The resonant tank parameters of L_r, L_p and C_r in Table 3 are used, and the peak power voltage gain requirement is satisfied at f_{r2}. With the designed parameters, simulation and experiments are performed and the performance of LLC OBC is observed.

III. SIMULATION VERIFICATION OF PFC STAGE

PSIM simulation is performed to verify the proposed LLC converter at both DC static operating points and AC-DC operation with PFC. According to the theoretical analysis, the whole AC line cycle (60Hz) should be implemented within the frequency between f_{r1} and f_{r2}. This section verifies the feasibility of voltage gain in DC-DC simulation with selected input and output DC voltage conditions.

A. DC-DC Static Simulation

Two AC-DC conditions are verified with DC operating point simulation: (1) 200V AC input to 430V DC output, which is the highest voltage gain requirement condition with lowest input and highest output. This condition is simulated to verify the voltage boosting ability of proposed parameters in PFC stage. (2) 240V AC input to 250V DC output condition, which is the lowest voltage gain requirement condition with lowest input and highest output. The output power is de-rated to 1250W with 5A load current at 250V in this condition. This condition is simulated to verify that the converter always operate between f_{r2} (350kHz) and f_{r1} (653kHz).

The phase from 10° to 90°are simulated. 90° to 170° operates the same 10° to 90°. So according to the simulation all the operating points from 10° to 170° could be implemented between f_{r2} and f_{r1}. Therefore, more than 90% of the AC input range can be achieved in the whole input and output voltage range.

Fig. 6 and Fig. 7 show the DC-DC static operating point verification waveforms. The minimum frequency and highest voltage gain condition is illustrated in Fig. 6, which corresponds to 10° condition of 200V AC input to 430V output. The switching frequency is 366kHz and the voltage gain is 11.85. The maximum frequency and lowest voltage gain condition is illustrated in Fig. 7, which corresponds to 90° condition of 240V AC input to 250V output. The switching frequency is 651kHz and the voltage gain is 1.0, this is also designed to be the resonant point of the LLC converter. In this condition it can be observed from the current waveform that resonant current is much higher than parallel inductor current, which indicates a peak load condition.
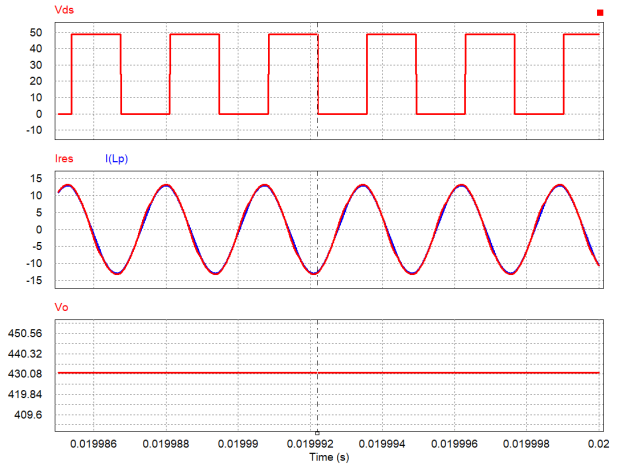

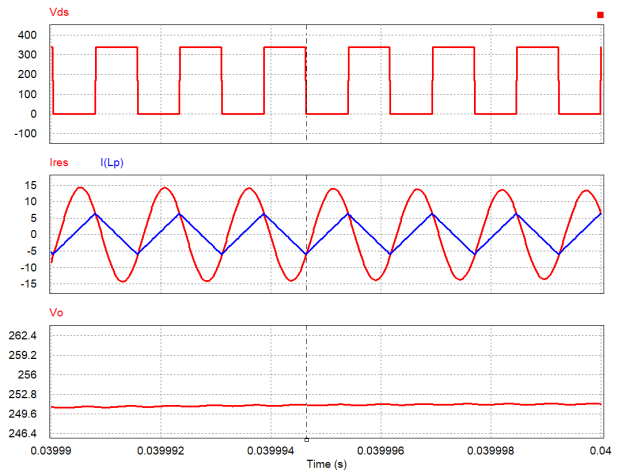Fig. 6.   Minimum frequency point: 200Vac @10° to 430V

Fig. 7.   Maximum frequency point: 240Vac @90° to 250V

It can be observed from the DC static operating point simulation that in the whole input and output range, the frequency is limited between f_{r1} and f_{r2}. Theoretically this guarantees the zero voltage switching on the primary side and the zero current switching on the secondary side. As shown in Fig. 6 and Fig. 7, the resonant current is always negative before the primary switches are turned on, therefore ZVS is achieved.

B. AC/DC Simulation with Power Factor Correction

With the static DC operating points verified in DC-DC converter model and 10° to 170° voltage regulation established, a simulation with AC-DC LLC converter for OBC application with PFC is built to validate the AC input performance. The maximum voltage gain operation is shown in Fig. 8 with 200V AC input and 430V DC output. 99.5% power factor and 5% total harmonic distortion (THD) are achieved. The double line frequency ripple V_{p-p} of output voltage indicates the high power factor. The amplitude of this voltage ripple is determined by (16):

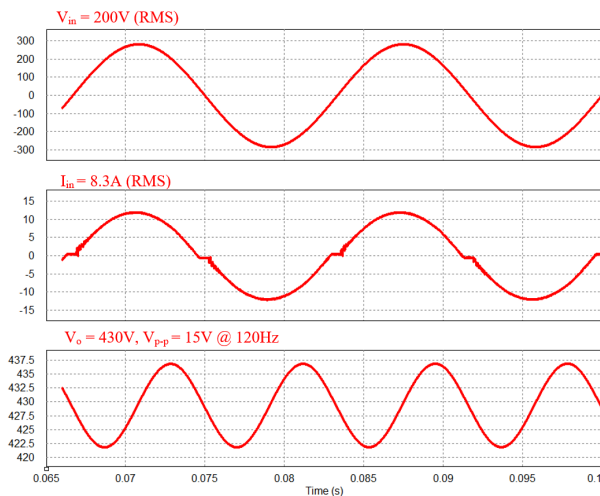$$V_{p-p} = \frac{P_o}{2\pi F C_o} \qquad (16)$$

4598

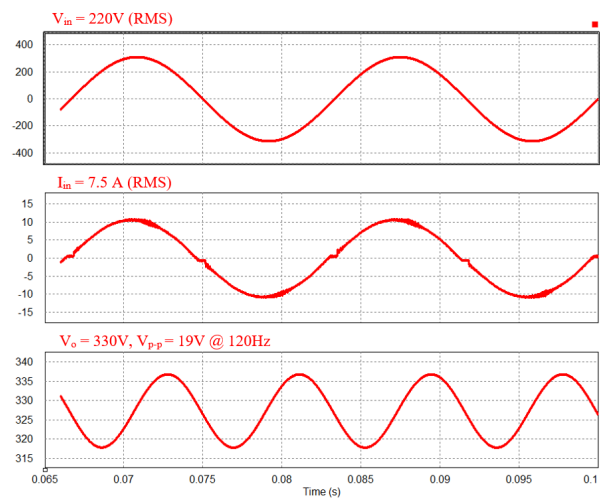Fig. 8. 200Vac to 430V output, PF = 99.5%, THD = 5.3%

Fig. 9. 220Vac to 330V output, PF = 99.3%, THD = 3.1%

Where F is the line frequency of AC input voltage, C_o is the output capacitance. The double line frequency ripple compensation of PFC will be investigated in the future to complete OBC implementation.

A nominal operation with 220V input and 330V output is shown in Fig. 9. 99.3% power factor and 3.1% total harmonic distortion (THD) are achieved in this condition. The double line frequency ripple of output voltage also indicates a good PFC performance. Therefore, the simulation verification shows the feasibility of developing LLC converter into AC-DC rectifier with PFC.

IV. EXPERIMENTAL TEST AND VERIFICATION

A laboratory prototype is built to verify the performance of proposed LLC AC/DC converter with power factor correction. The schematic is shown in Fig. 10 and photo of prototype is shown in Fig. 11, 2.2 kW/L power density achieved by this converter with liquid cooling assembly, 2.9kW/L without EMI filter is achieved. In the experimental verification, DC-DC static operating points are firstly tested, and then the AC/DC operation with PFC with the target range of input and output voltage is performed.
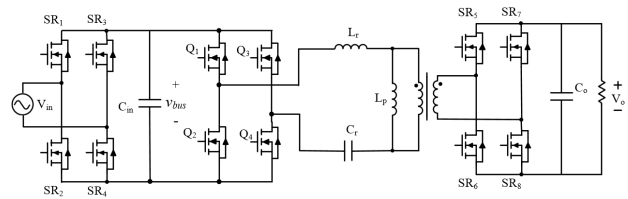

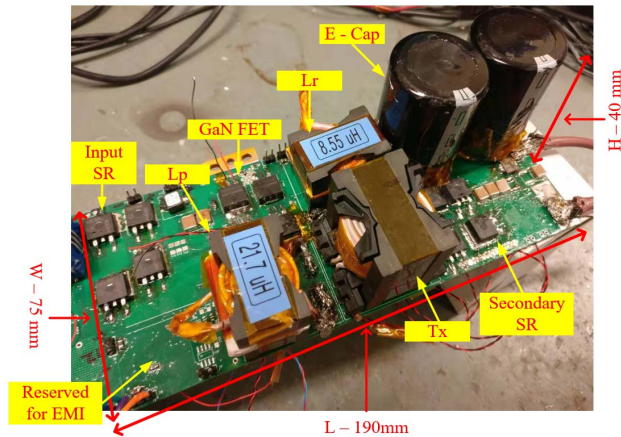Fig. 10. Schematic of AC-DC LLC converter with PFC

Fig. 11. Top view of 1650W AC-DC LLC converter prototype

To verify the quasi-static operating points of PFC stage and voltage boosting capability, DC-DC operating points are tested on the proposed LLC converter. Especially at low phase angle and light load conditions, the input voltage is low, and the output voltage should keep the same, requiring a high voltage gain. The high load conditions with high input voltage and small load resistance are also tested.

Fig. 12 shows the case when input voltage is 200V and output voltage is 330V at 5A load current. The Gan FET gate voltage V_{gs}, Drain to Source voltage V_{ds} and the resonant current waveforms at 45° phase are shown. The DC-DC operating condition at 45° has the same output power as AC input condition and the performance can approximately indicate the actual AC-DC performance. The operation can be implemented with 98.0% efficiency.
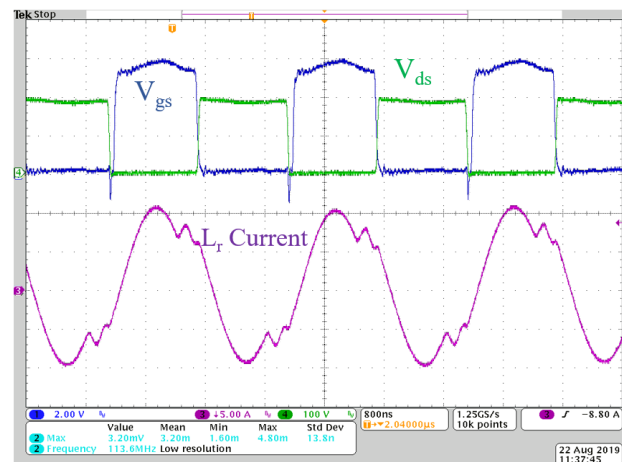

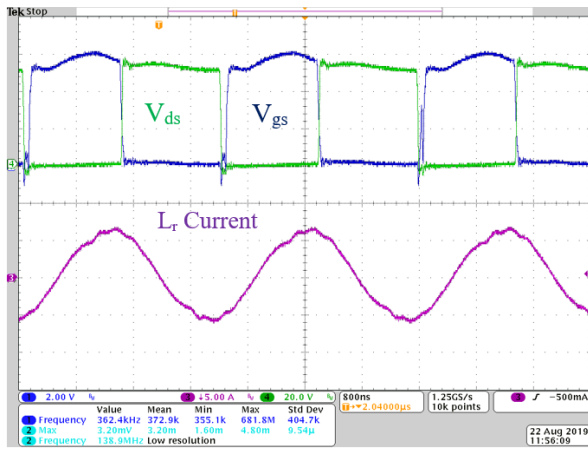Fig. 12. 200V input to 330V/5A output (200Vac @ 45°)

4599

Fig. 13. 49V input to 380V output (200Vac @ 10°)

Light load DC-DC experiment is also performed to verify the voltage regulation feasibility of LLC converter at high voltage gain condition. Fig. 13 illustrates the 10° phase angle condition of 200V AC input (49V DC voltage) with 380V output voltage, the output power is 100W. With higher available maximum voltage gain at light load condition, the voltage gain requirement (G_{req} = 10.5) is achieved and output voltage is regulated. The switching frequency is limited between f_{r1} and f_{r2}, so that voltage zero crossing of GaN FETs is still guaranteed.

For AC-DC operation, the input RMS voltage ranges from 200V to 240V, output DC voltage is from 250V to 430V. Constant power of 1650W is required with 330V to 430V output condition, constant 5A load current is applied for 250V to 330V output voltage. The AC-DC power conversion stage with power factor correction is tested to verify the PF performance and single stage converter efficiency. The input rectifier is using MOSFET synchronized rectifier, the output rectifier is using SiC diode bridge.

Fig. 14 shows the AC-DC stage with PFC waveforms with 220Vac input voltage and 250V output DC voltage at 5A load current condition. This is the derated condition of PFC operation, the output power is 1.2kW, the power factor of this condition is 99.3% and the efficiency is 96.9%. This testing result verifies the AC-DC operation with PFC at low output voltage condition with high switching frequency.

Fig. 15 shows the condition with 230Vac input voltage and 320V output DC voltage at 5A load current condition, this is the nominal operation of PFC stage, the load current is still at the highest value. The power factor is 99.1% and the efficiency is 96.9%.

Fig. 16 shows the full output voltage condition at 380V DC output and 1.53kW, the load current is derated to 4A to implement a constant output power. The power factor is 98.7% and the efficiency is 96.6%. Thus, the AC-DC operation at high output voltage condition and low switching frequency is also achieved with power factor correction.

The experimental results verify the theoretical analysis of using a single stage LLC converter to achieve AC-DC operation with power factor correction for OBC application.

In the tested input and output conditions, the input current is well regulated to be sinusoidal waveform, high power factor and low THD are achieved. The switching frequency is limited between f_{r1} and f_{r2}, so zero voltage switching is achieved with GaN FETs. LLC converter with Synchronous rectifier MOSFET instead of SiC diode is also tested, and full load efficiency is improved by 0.2%. Therefore, the overall efficiency of AC-DC operation with power factor correction at 230V input and 320V/5A output can achieve over 97%.
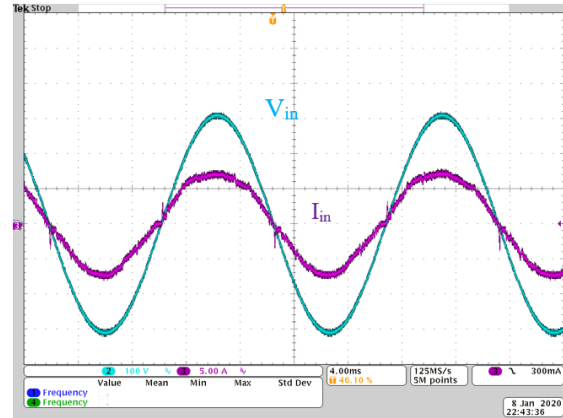

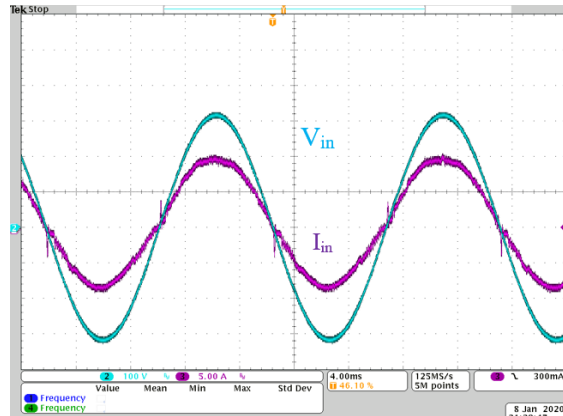Fig. 14. PFC waveform at 220V AC input to 250V/5A DC output

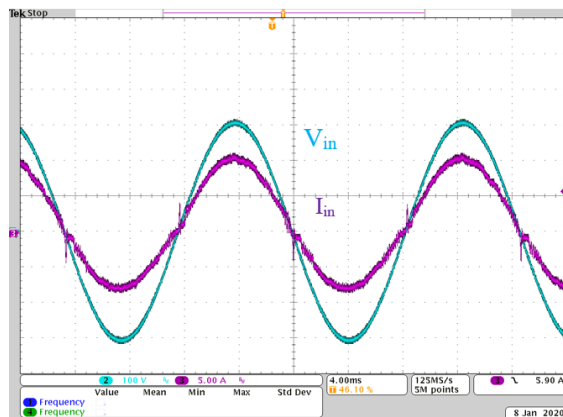Fig. 15. PFC waveform at 220V AC input to 320V/5A DC output

Fig. 16. PFC waveform at 230V AC input to 380V/4A DC output

4600

V. Conclusion

This chapter discusses the development of a single stage LLC converter into an AC-DC converter with power factor correction for OBC application. A design criterion regarding voltage gain requirement of the full input AC line cycle is analyzed. According to the voltage gain analysis, the maximum gain of LLC converter is significantly increased at light load condition, which matches with the gain requirement of AC-DC converter with PFC. This chapter proves that PFC can be well implemented if the full load voltage gain is maintained at the low resonant frequency f_{r2}. Based on this design requirement, an LLC AC-DC converter with PFC for OBC application is designed and an experimental prototype is built. The experimental results verify the high power factor, high efficiency and high power density on the proposed LLC converter with PFC.

References

[1] A. Khaligh and M. D'Antonio, "Global Trends in High-Power On-Board Chargers for Electric Vehicles," in IEEE Transactions on Vehicular Technology, vol. 68, no. 4, pp. 3306-3324, April 2019.

[2] R. Hou and A. Emadi, "A Primary Full-Integrated Active Filter Auxiliary Power Module in Electrified Vehicles with Single-Phase Onboard Chargers," IEEE Transactions on Power Electronics, vol. 32, no. 11, pp. 8393-8405, 2017.

[3] R. Hou and A. Emadi, "Applied Integrated Active Filter Auxiliary Power Module for Electrified Vehicles with Single-Phase Onboard Chargers," IEEE Transactions on Power Electronics, vol. 32, no. 3, pp. 1860-1871, 2017.

[4] D. Moon, J. Park and S. Choi, "New interleaved current-fed resonant converter with significantly reduced high current side output filter for EV and HEV applications," IEEE Transactions on Power Electronics, vol. 30, no. 8, pp. 4264-4271, Aug. 2015.

[5] D. Hamza, M. Pahlevaninezhad, and P. K. Jain, "Implementation of a novel digital active EMI technique in a DSP-based dc–dc digital controller used in electric vehicle (EV)," IEEE Transactions on Power Electronics, vol. 28, no. 7, pp. 3126-3137, Jul. 2013.

[6] C. M. Lai and K. K. Shyu, "A single-stage AC/DC converter based on zero voltage switching LLC resonant topology," IET Electric Power Applications, vol. 1, no. 5, pp. 743-752, 2007.

[7] H. L. Do and B. H. Kwon, "Single-stage asymmetrical PWM AC-DC converter with high power factor," IEE Proceedings - Electric Power Applications, vol. 149, no. 1, pp. 1-8, 2002.

[8] K. Seong-Ju, K. Choon-Taek, K. Young-Jo, L. Jae-Du, and K. Young-Seok, "Single-stage asymmetrical LLC resonant converter with low voltage stress across switching devices," in 2013 International Conference on Electrical Machines and Systems (ICEMS), 2013, pp. 1771-1775.

[9] J. Lu et al., "A Modular Designed Three-phase High-efficiency High-power-density EV Battery Charger Using Dual/Triple-Phase-Shift Control," IEEE Transactions on Power Electronics, vol. PP, no. 99, pp. 1-1, 2017.

[10] J. Lu et al., "Applying Variable-Switching-Frequency Variable-Phase-Shift Control and E-Mode GaN HEMTs to an Indirect Matrix Converter-Based EV Battery Charger," IEEE Transactions on Transportation Electrification, vol. 3, no. 3, pp. 554-564, 2017.

[11] M. Alam, W. Eberle, D. S. Gautam and C. Botting, "A Soft-Switching Bridgeless AC–DC Power Factor Correction Converter," in IEEE Transactions on Power Electronics, vol. 32, no. 10, pp. 7716-7726, Oct. 2017.

[12] D. L. O. Sullivan, M. G. Egan, and M. J. Willers, "A Family of Single-Stage Resonant AC/DC Converters With PFC," IEEE Transactions on Power Electronics, vol. 24, no. 2, pp. 398-408, 2009.

[13] Y. Qiu, W. Liu, P. Fang, Y. Liu and P. C. Sen, "A mathematical guideline for designing an AC-DC LLC converter with PFC," 2018 IEEE Applied Power Electronics Conference and Exposition (APEC), San Antonio, TX, 2018, pp. 2001-2008

[14] Z. Hu, Y. Qiu, Y.-F. Liu, and P. C. Sen, "A Control Strategy and Design Method for Interleaved LLC Converters Operating at Variable Switching Frequency," Power Electronics, IEEE Transactions on, vol. 29, no. 8, pp. 4426-4437, 2014.

[15] Z. Hu, Y. Qiu, L. Wang, and Y.-F. Liu, "An Interleaved LLC Resonant Converter Operating at Constant Switching Frequency," Power Electronics, IEEE Transactions on, vol. 29, no. 6, pp. 2931-2943, 2014.

[16] R. L. Steigerwald, "A comparison of half-bridge resonant converter topologies," IEEE Transactions on Power Electronics, vol. 3, no. 2, pp. 174-182, 1988.

[17] S. D. Simone, C. Adragna, C. Spini, and G. Gattavari, "Design-oriented steady-state analysis of LLC resonant converters based on FHA," in International Symposium on Power Electronics, Electrical Drives, Automation and Motion, 2006. SPEEDAM 2006., 2006, pp. 200-207.

[18] Z. Hu, L. Wang, Y. Qiu, Y.-F. Liu, and P. C. Sen, "An Accurate Design Algorithm for LLC Resonant Converters Part II," IEEE Transactions on Power Electronics, vol. 31, no. 8, pp. 5448-5460, 2016.

[19] Z. Hu, Y. F. Liu, and P. C. Sen, "Cycle-by-cycle average input current sensing method for LLC resonant topologies," in 2013 IEEE Energy Conversion Congress and Exposition, 2013, pp. 167-174.

[20] Y. Qiu, L. Wang, H. Wang, Y. Liu, and P. C.Sen, "Bipolar Ripple Cancellation Method to Achieve Single-Stage Electrolytic-Capacitor-Less High-Power LED Driver," Emerging and Selected Topics in Power Electronics, IEEE Journal of, vol. 3, no. 3, pp. 698-713, 2015.

[21] Y. Qiu, H. Wang, Z. Hu, L. Wang, Y.-F. Liu, and P. C. Sen, "Electrolytic-Capacitor-Less High-Power LED Driver," in Energy Conversion Congress and Exposition (ECCE), 2014 IEEE, 2014, pp. 3612-3619.

[22] Z. Liu, B. Li, F. C. Lee and Q. Li, "Design of CRM AC/DC converter for very high-frequency high-density WBG-based 6.6kW bidirectional on-board battery charger," 2016 IEEE Energy Conversion Congress and Exposition (ECCE), Milwaukee, WI, 2016, pp. 1-8.

[23] Z. Liu, B. Li, F. C. Lee and Q. Li, "High-Efficiency High-Density Critical Mode Rectifier/Inverter for WBG-Device-Based On-Board Charger," in IEEE Transactions on Industrial Electronics, vol. 64, no. 11, pp. 9114-9123, Nov. 2017.